RESEARCH PAPER

Mathematical modelling and simulation of microbial carbonate precipitation: the urea hydrolysis reaction

Hitoshi Matsubara[1] 🆔 · Tomonori Yamada[2]

Abstract

Microbial carbonate precipitation is expected to play a major role in next-generation soil improvement technologies. To date, research into this method has relied on experimental and/or observational approaches. However, in order to understand the long-term effects of microbial carbonate precipitation and apply these to real environments, it is necessary to employ a predictive approach to determine the future state of the soil when using this soil improvement method. In this work, a mathematical model and numerical simulations based on the reaction–diffusion system for the microbial urea hydrolysis reaction are proposed. These techniques may be used to provide the spatiotemporal precipitation patterns of carbonates between soil particles and the particle surfaces. The simulation results revealed that the characteristic precipitation patterns depend on the diffusion of carbonates caused by the microbial urea hydrolysis reaction, and there was a significant shift in the amount of carbonate from a dissipated state into an equilibrium state.

Keywords Microbial carbonate precipitation · Reaction–diffusion-based modelling · Spatiotemporal precipitation pattern · Urea hydrolysis reaction

1 Introduction

Mathematical modelling and numerical simulations of the mechanical behaviour of naturally occurring materials have enabled the prediction of various environmental phenomena, including geological changes [20]. With these advances in prediction technologies, unstable ground behaviour due to a sudden or temporary main cause, such as a localized torrential downpour and/or an earthquake, becomes predictable to a certain extent [5, 7, 26, 28]. Geomaterials, however, are also subject to particular chemical and biological reactions that affect any related precipitation and weathering processes [31, 52]. Therefore, in

✉ Hitoshi Matsubara
    matsbara@tec.u-ryukyu.ac.jp

1   School of Civil Engineering, University of the Ryukyus, Nishihara, Okinawa, Japan

2   Department of Systems Innovation, The University of Tokyo, Bunkyo, Tokyo, Japan

considering long-term changes in geo-materials using mathematical prediction techniques, it is also essential to know the future soil conditions.

Soil improvement technologies have been developed experimentally and empirically from a variety of viewpoints, such as geotechnical engineering, geomechanics, chemodynamics, and microbiology [3]. There are more than 40,000 projects worldwide related to soil improvement technologies [18]. Although there are many engineering techniques used in soil improvement technologies [25, 27, 44], the new approach of bio-mediated soil improvement technology deserves special attention. It has been observed through various experimental shearing tests and investigations that the shear strength of microbial-mediated soils can be improved using the process of biochemical cementation [9, 11, 15, 17, 18, 23, 45, 48, 51]. For this reason, this microbial phenomenon is expected to become the focus of innovative techniques for use in next-generation soil improvement technologies.

The biochemical cementation phenomenon may also be observed in a natural environment [39, 42]. The cementation may be fostered in natural environments through the microbially induced cation generation of carbonate dissolution and subsequent carbonate precipitation [36]. Also,

the cementation depends on environmental parameters such as temperature and pH values [9, 45]. Thus, microbially induced cementation in geo-materials is of interest from an engineering viewpoint because there is a possibility that this may be applied artificially to natural environments. In contrast, predicting inner structural changes is essential in understanding the cementation mechanism because the reformation of the inner structure of soil directly influences the increase in macroscopic strength of the soil. However, this can be difficult in practice because we may not be able to change certain parameters easily with respect to the microbial activity. Hence, common practice has been to search for different microbes and define the appropriate environmental conditions such as by trial and error through a large number of experiments and observations using microscopes, such as a scanning electron microscope, a transmission electron microscope, and X-ray microtomography. Particularly, X-ray microtomographic investigations have served towards understanding of the evolution of inner microbially induced structures [14, 19, 46, 47]. This technique has permitted direct observation of a real geometry of active calcite bond structures which bridges neighbouring grains and an inactive calcite bond. As a result, this technique has revealed the relevance between micro-organisms in soil and the intrinsic material properties such as void structure and grain distribution [47].

The evolution and inner structures of bio-mediated soil depend on the metabolic pathways of the microbes, bio-mediated changes in the minerals in the soil, and microbial behaviour [17, 51]. In the case of the microbial urea hydrolysis reaction, one of the processes of bio-mediated soil improvement, carbonate precipitations are facilitated by microbial activity in the soil. Various alkalophilic soil bacteria consume urea and decompose it into ammonia and carbon dioxide. Subsequently, the carbon dioxide dissolves into the ground water, carbonate ions in the ground react with calcium ions, and consequently calcite is precipitated at the boundaries of soil particles and on their surfaces [11]. Although there are other pathways for microbial carbonate precipitation (MCP), such as photosynthesis, denitrification, ammonification, sulphate reduction, and methane oxidation [6, 16, 49, 55], the microbial urea hydrolysis reaction is worthy of attention because the reaction occurs efficiently under the influence of natural environmental factors with relatively little time and light/heavy equipment is not needed [10, 15, 18, 38]. That is, this reaction may be suitable for practical application. Nevertheless, studies on the microbial urea hydrolysis reaction have so far relied on experimental and/or observational approaches. In order to understand the long-term effects of MCP and to apply these to natural environments, it is necessary to develop a predictive technique that can

determine the future state of the soil when using soil improvement technologies.

Several prediction techniques have been proposed in order to describe the dynamics of granular materials (e.g. [7, 8, 12, 28, 29, 53]). For example, Więckowski [53] formulated the material point method for granular material simulation, in which a large deformation simulation, such as may be used to describe granular flow in a silo, was conducted macroscopically. Additionally, the fracture behaviour of clean sand under biaxial tests was also simulated microscopically using the discrete element method [29]. In contrast, there are very few studies on the simulation of MCP. Fauriel and Laloui [21] proposed a novel mechanical model that considered bio-chemo-hydraulic reactions in order to describe microbial-induced calcium precipitation in soils. Although this kind of model allows the prediction of macroscopic mechanical behaviour, the precipitation process and mechanism related to centralization on soil particles of microbially induced calcium carbonates may not be analysed [1, 21]. This is because the model was formulated from a macroscopic point of view, treating the voids in a soil sample as a variable of its porosity. A bio-cemented simulation based on the discrete element method has also been proposed [22], allowing the simulation of certain MCP granular material fracture behaviours. However, this technique may be not suitable for understanding biochemical precipitation patterns at the soil particle scale as this technique was designed for mechanical strength analysis. A methodology for understanding the patterns and mechanisms related to filling the void structure in sandy soils has not yet been established.

In this work, we attempt to bring a new perspective to the bio-mediated soil improvement technology field, drawing on mathematical modelling and simulation techniques in order to understand the mechanism of microstructural formation and predict the future state of the soil. We describe spatial precipitation patterns obtained using the proposed mathematical model at the soil particle scale and discuss MCP processes on the microscopic level.
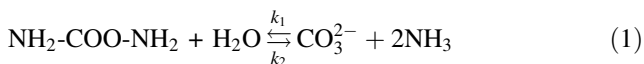
2 A mathematical model for microbial urea hydrolysis reaction

2.1 Mathematical formulation

In the field of theoretical biology, it is well known that certain characteristics of bacterial colonies growing on agar plates can be accurately described by a mathematical interaction system based on the reaction–diffusion equation (e.g. [24, 34]). The essential assumption contained in this mathematical model is the introduction of an internal state concept to the reaction–diffusion system [4, 35]. Applying

this concept, if the internal state is increased, bacteria actively move and grow, whereas if it is decreased, the bacteria become inactive [35]. Another mathematical model for understanding the bacterial growth on agar pates is the lubricating bacteria model, which explains certain complex colony patterns using the effects of interaction variables defined by their bacterial concentration, the height of the lubrication layer, nutrition, and the presence of stationary bacteria [13, 32]. However, applying these models directly to the urea hydrolysis reaction may be inappropriate as these models do not support phenomena related to MCP. The most important requirement for the urea hydrolysis reaction is that calcium carbonates are precipitated in a metabolic reaction in urea-splitting bacteria [17]. Hence, in formulating a mathematical model to describe the microbial urea hydrolysis reaction, the model must allow for this metabolic reaction.

MCP that is due to the urea hydrolysis reaction corresponds to the following expressions [16]:

$$NH_2\text{-}COO\text{-}NH_2 + H_2O \underset{k_2}{\overset{k_1}{\rightleftharpoons}} CO_3^{2-} + 2NH_3 \tag{1}$$

$$Ca^{2+} + CO_3^{2-} \underset{k_4}{\overset{k_3}{\rightleftharpoons}} CaCO_3 \downarrow \tag{2}$$

where k_1, k_2, k_3, and k_4 are the reaction rate constants. Eq. (1) relates to the microbial urea hydrolysis reaction, and Eq. (2) relates to the chemical precipitation of calcite particles. In this work, these biochemical equations are formulated in accordance with the reaction–diffusion system [50]. Since 1993, when the processes of 'birth' and 'death' in living creatures were simulated in a simple system based on a reaction–diffusion system [33, 40], this system has been recognized as a mathematical model that also represents bacterial movements and growth [30, 34]. Hence, a mathematical model that defines microbial urea hydrolysis is an appropriate selection for the present study.

Considering the diffusion and inflow terms in the biochemical reactions [Eqs. (1) and (2)], a mathematical model based on the reaction–diffusion system may be described as follows:

$$\frac{\partial \mathbf{A}}{\partial t} = \frac{\partial}{\partial \mathbf{x}} D_A \frac{\partial \mathbf{A}}{\partial \mathbf{x}} - k_1 \mathbf{AB} + k_2 \mathbf{C}_i \mathbf{E}^2 + \mathbf{A}_{in} \tag{3}$$

$$\frac{\partial \mathbf{B}}{\partial t} = \frac{\partial}{\partial \mathbf{x}} D_B \frac{\partial \mathbf{B}}{\partial \mathbf{x}} - k_1 \mathbf{AB} + k_2 \mathbf{C}_i \mathbf{E}^2 + \mathbf{B}_{in} \tag{4}$$

$$\frac{\partial \mathbf{C}_i}{\partial t} = \frac{\partial}{\partial \mathbf{x}} D_{C_i} \frac{\partial \mathbf{C}_i}{\partial \mathbf{x}} + k_1 \mathbf{AB} - k_2 \mathbf{C}_i \mathbf{E}^2 - k_3 \mathbf{C}_i \mathbf{F}_i + k_4 \mathbf{P} \tag{5}$$

$$\frac{\partial \mathbf{E}}{\partial t} = \frac{\partial}{\partial \mathbf{x}} D_E \frac{\partial \mathbf{E}}{\partial \mathbf{x}} + k_1 \mathbf{AB} - k_2 \mathbf{C}_i \mathbf{E}^2 \tag{6}$$

$$\frac{\partial \mathbf{F}_i}{\partial t} = \frac{\partial}{\partial \mathbf{x}} D_{F_i} \frac{\partial \mathbf{F}_i}{\partial \mathbf{x}} - k_3 \mathbf{C}_i \mathbf{F}_i + k_4 \mathbf{P} + \gamma \mathbf{F}_i \tag{7}$$

$$\frac{\partial \mathbf{P}}{\partial t} = k_3 \mathbf{C}_i \mathbf{F}_i - k_2 \mathbf{P} \tag{8}$$

where $\mathbf{A}$, $\mathbf{B}$, $\mathbf{C}_i$, $\mathbf{E}$, $\mathbf{F}_i$, and $\mathbf{P}$ denote the concentrations of $NH_2\text{-}COO\text{-}NH_2$, H_2O, CO_3^{2-}, NH_3, Ca^{2+}, and $CaCO_3$, respectively. These variables are functions of time and space. D_* is the diffusion coefficient of the related variable $*$, and these have spatially random values. The inflow terms $\mathbf{A}_{in}$ and $\mathbf{B}_{in}$ are the constant amounts of $NH_2\text{-}COO\text{-}NH_2$ and H_2O, respectively. These terms take into account the inflow of and from outside environments. $\gamma \mathbf{F}_i$ is the inflow term for Ca^{2+} and is the constant coefficient. It is known that bacteria have extrusion mechanisms called as bacterial Ca^{2+} pump to maintain low concentrations of intracellular calcium [41]. The Ca^{2+} adsorption to the cell surface of bacteria by the Ca^{2+} pump promotes heterogeneous nucleation of calcite, and particularly in the media with high enough concentrations of Ca^{2+} ions, the bacteria promote the precipitation of calcite [43]. This metabolism may also occur in MICP process because the majority of MICP-related works have used calcium concentrations in the range of 0.1–1 mol/L that are taken for calcium chloride as a source [17]. Hence, this inflow term ($\gamma \mathbf{F}_i$) in Eq. (7) aims to capture this extrusion mechanism in the proposed model.

The proposed mathematical model represents a completely open system characterized by the interaction of six elements associated with all variables. The diffusion of $CaCO_3$ is not considered in this model because $CaCO_3$ is a solid material and may not be diffused. If an adequate amount of urea is present in this model, and water and calcium ions are supplied in the analytical region, calcite would be generated constantly at pore space and on surfaces of soil particles. That is, the proposed model has been formulated based on the following hypotheses:

Hypothesis 1: Precipitation of calcium carbonates occurs randomly in any part of pore space from some nucleation points that remain fixed.

Hypothesis 2: Precipitation and growth of calcium carbonates occur under constant supersaturation sate.

Whereas particles migration by groundwater advection, adsorption and deposition on the grain surface are not considered in the mathematical formulation. It is noted that the focus in this study is put on precipitation patterns such as bridging neighbouring particles which precipitate randomly in the pore space.

2.2 Discretization

In the current study, the diffusion operators of Eqs. (3)–(8) are discretized using the finite difference scheme. Let us consider the following equation using a variable G and a coefficient D.

$$\frac{\partial G}{\partial t} = \nabla(D\nabla G) = \nabla D\nabla G + D\nabla^2 G \qquad (9)$$

Here, the left side may be discretized using the forward Euler integrations, and the first term on the right side is divided into two terms, and each term can be discretized using the forward difference and reverse difference, respectively. That is,

$$\frac{\partial G}{\partial t} = \frac{1}{2}\nabla D\nabla G + \frac{1}{2}\nabla D\nabla G + D\nabla^2 G \qquad (10)$$

in a natural environment, numerous parametric studies may be needed. Thus, each parameter is considered as a dimensionless variable, and the morphological characteristics of the inner sands and the trends of each dimensionless concentration are discussed in the current study.

The system ($x \times y \times z$), grid size, and number of grid points are $2 \times 1 \times 1$, 0.0156, and 545,025, respectively. The time increment (Δt) was set to 0.1, and the diffusion coefficients were randomly chosen to be $D_A = 5e-7 \sim 5e-5$ and $D_B = D_{C_i} = D_E = D_{F_i} = 7e-7 \sim 7e-5$. The Neumann boundary conditions were set to all of the surfaces, and two spherical soil particles (radius 0.7 and 0.45), in which the microbial urea hydrolysis reaction does not occur, were arranged as shown in Fig. 1. In the numerical simulations, an adequate amount of urea and water were supplied constantly at the three points in the analytical region (see Fig. 1), $A_{in} = B_{in} = 0.5 \sim 1.0$ were set in a random manner in Eqs. (3) and
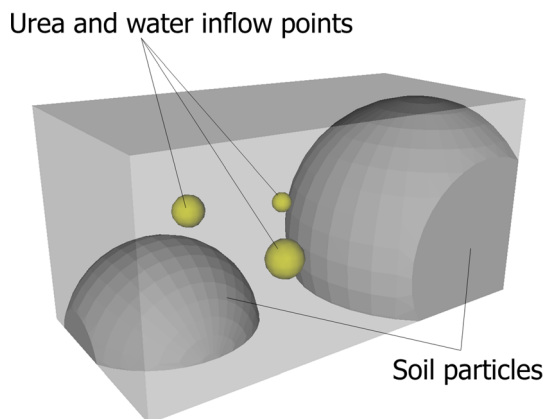
$$\frac{G_i^{n+1} - G_i^n}{\Delta t} = \frac{(D_{i+1} + D_i)G_{i+1}^n - (D_{i+1} + 2D_i + D_{i-1})G_i^n + (D_i + D_{i-1})G_{i-1}^n}{2\Delta x^2} \qquad (11)$$

where n is the number of the time step, i is the grid number, Δt is the time increment, and Δx is the grid size.

3 Numerical simulation results

3.1 Simulation models

Numerical simulations are conducted for a three-dimensional cuboid. In order to quantitatively obtain the concentration of each element and numerically express MCP
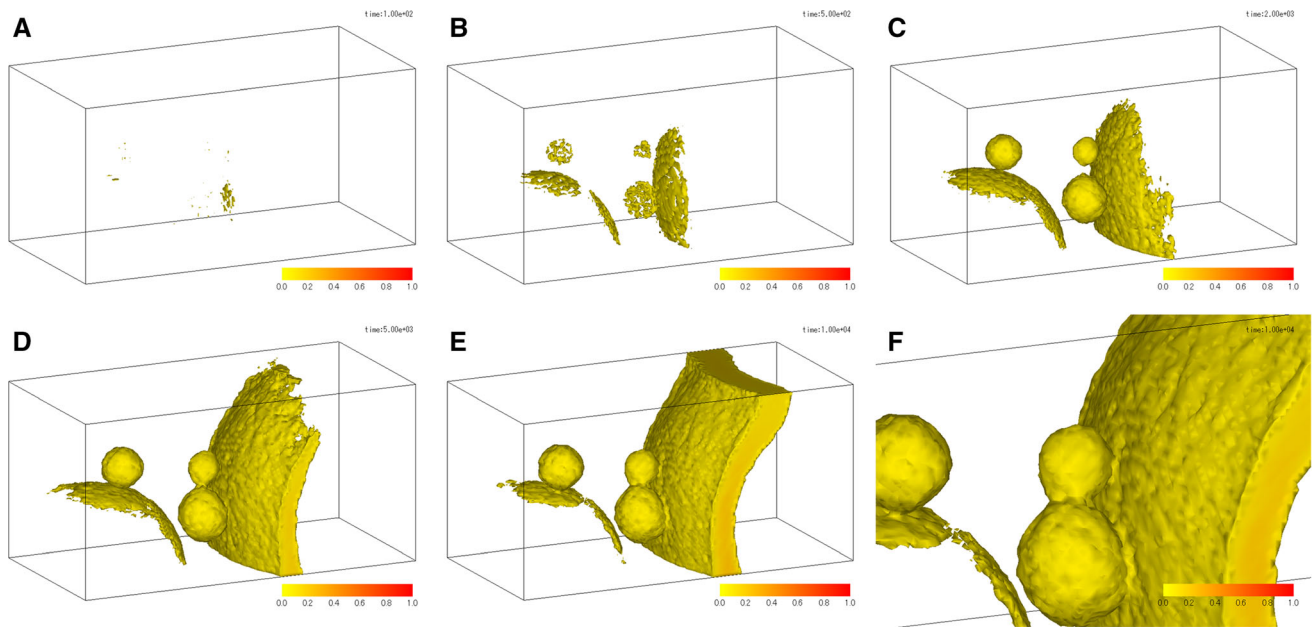
(4) throughout the period of analysis. The γ variable in Eq. (7) was set to 0.005.

The amount of calcite and its precipitation patterns were investigated through various numerical simulations. The entire analytical region was initially placed in the disordered state with a low number of elements, namely $A = B = C_i = E = F_i = 0.0 \sim 0.05$, where the numbers were chosen randomly. Subsequently, the cases with various reactant rate constants on Eqs. (3)–(8) were tested, and the differences in the results determined.

3.2 Simulation results

Figure 2 shows the evolution of a calcite precipitation pattern in the case of $k_1 = 25$, $k_2 = 0.005$, $k_3 = 10$, and $k_4 = 0.005$. In the initial stage, the calcite precipitates around the urea and water inflow points and subsequently the calcite particles distribute among the particle boundaries and on the particle surfaces simultaneously. Then, the precipitates eventually connect with each other [see Movies (1a) and (1b)]. The evolution of bond diameter as result of continuous precipitation has also been observed in several experiments [17, 18]. Therefore, the proposed model may be suitable qualitatively for MCP with urea hydrolysis reaction.

Simulations were conducted without using the diffusion terms in Eqs. (3)–(7), that is, by using the reaction equations. Figure 3 shows the evolution of calcite precipitation in the case of a non-diffusion-type model. Calcite

Fig. 1 The numerical simulation model. Two spherical soil particles (radius: 0.7 and 0.45) and three urea and water inflow points are located in the domain

Urea and water inflow points

Soil particles

Fig. 2 The evolution of calcite precipitations by the proposed mathematical model ($k_1 = 25$, $k_2 = 0.005$, $k_3 = 10$, and $k_4 = 0.005$). The times t at which the figures were taken are as follows: **a** $t = 1 \times 10^2$; **b** $t = 5 \times 10^2$; **c** $t = 2 \times 10^3$; **d** $t = 5 \times 10^3$; **e** $t = 1 \times 10^4$; and **f** $t = 1 \times 10^4$ [zooming of (**e**)]. The colour bar indicates the calcite concentration; red corresponds to a higher concentration (= 1.0) and light yellow to a lower concentration (= 0.0) (color figure online)
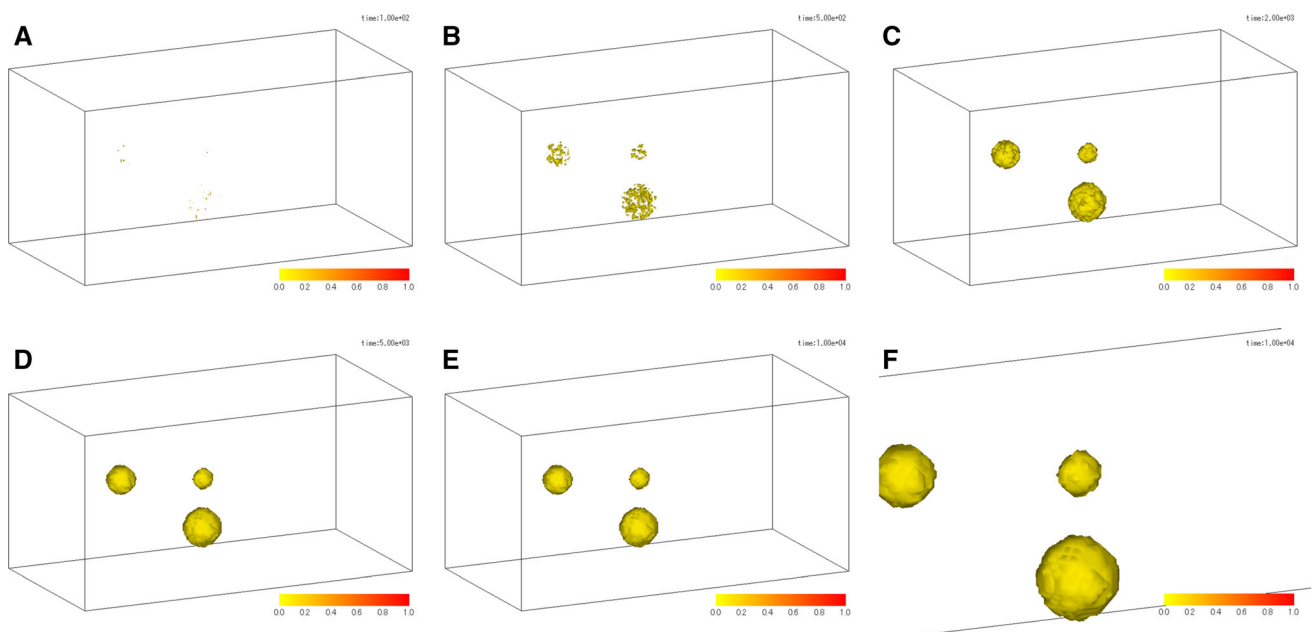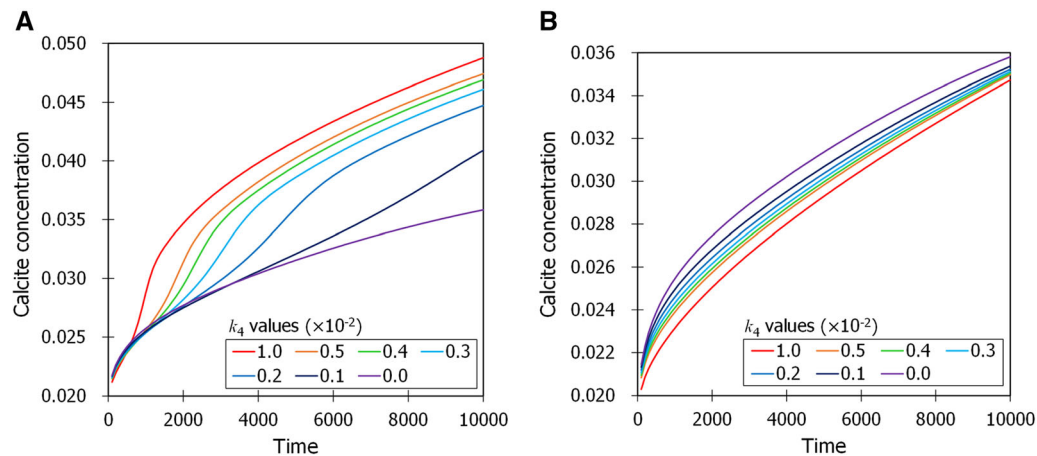

Fig. 3 The evolution of calcite precipitations by the non-diffusion model ($k_1 = 25$, $k_2 = 0.005$, $k_3 = 10$, and $k_4 = 0.005$). The times t at which the figures were taken are as follows: **a** $t = 1 \times 10^2$; **b** $t = 5 \times 10^2$; **c** $t = 2 \times 10^3$; **d** $t = 5 \times 10^3$; **e** $t = 1 \times 10^4$; and **f** $t = 1 \times 10^4$ [zooming of (**e**)]. The colour bar indicates the calcite concentration; red corresponds to a higher concentration (= 1.0) and light yellow to a lower concentration (= 0.0) (color figure online)

precipitation was not observed on the particle surfaces, with only a sparse calcite precipitation present at the urea inflow points [see Movies (2a) and (2b)].

Figure 4 shows the variations in calcite concentration in the whole analytical domain for different simulation times.

In Fig. 4a, the calcite concentration increased significantly as the value of k_4 decreased for $k_1 \leq k_3$. On the other hand, where $k_1 > k_3$ (see Fig. 4b), the calcite concentration decreased as the value of k_4 decreased, and the significant shift in the calcite concentration was not observed.

Fig. 4 The variation of calcite concentration with time using the proposed mathematical model. **a** The case of $k_1 = 25$, $k_2 = 0.005$, and $k_3 = 10$; **b** the case of $k_1 = 10$, $k_2 = 0.005$, and $k_3 = 25$. In the both cases, the values of k_4 are set to 1.0×10^{-2}, 0.5×10^{-2}, 0.4×10^{-2}, 0.3×10^{-2}, 0.2×10^{-2}, 0.1×10^{-2}, and 0.0
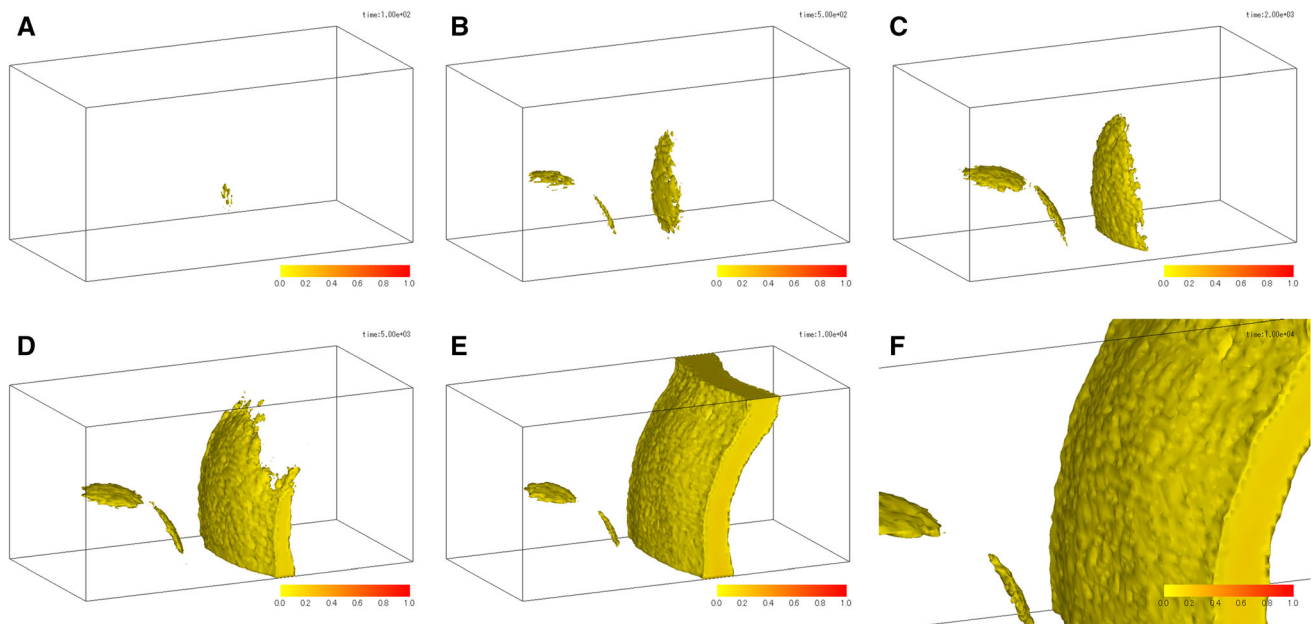

Fig. 5 The evolution of calcite precipitations by the proposed model ($k_1 = 10$, $k_2 = 0.005$, $k_3 = 25$, and $k_4 = 0.005$). The times t at which the figures were taken are as follows: **a** $t = 1 \times 10^2$; **b** $t = 5 \times 10^2$; **c** $t = 2 \times 10^3$; **d** $t = 5 \times 10^3$; **e** $t = 1 \times 10^4$; and **f** $t = 1 \times 10^4$ [zooming of (**e**)]. The colour bar indicates the calcite concentration; red corresponds to a higher concentration (= 1.0) and light yellow to a lower concentration (= 0.0) (color figure online)

In addition, Fig. 5 shows the calcite precipitation pattern for $k_1 > k_3$. The precipitation on the particle surfaces was also observed as well as in the case where $k_1 \leq k_3$ (see Fig. 2), but no precipitation between the soil particles occurred [see Movies (3a) and (3b)]. The calcite concentration variations in the non-diffusion-type model are shown in Fig. 6. Also, several significant shifts were observed in this case.

4 Discussion

The proposed mathematical model provides microscopic MCP patterns in soil (Figs. 2, 3, and 5). Figure 7 shows the MCP features recently observed in laboratory experiments on sandy soils [17]. From this figure, it may be seen that the precipitation proceeds from the surface of the soil particles and bonds to other particles. In addition, it is known that carbonate precipitation is created at contact points between soil particles taking advantage of urea hydrolysis catalysed by bacteria [11, 17, 37, 54]. From Figs. 2, 5, and 7c, a
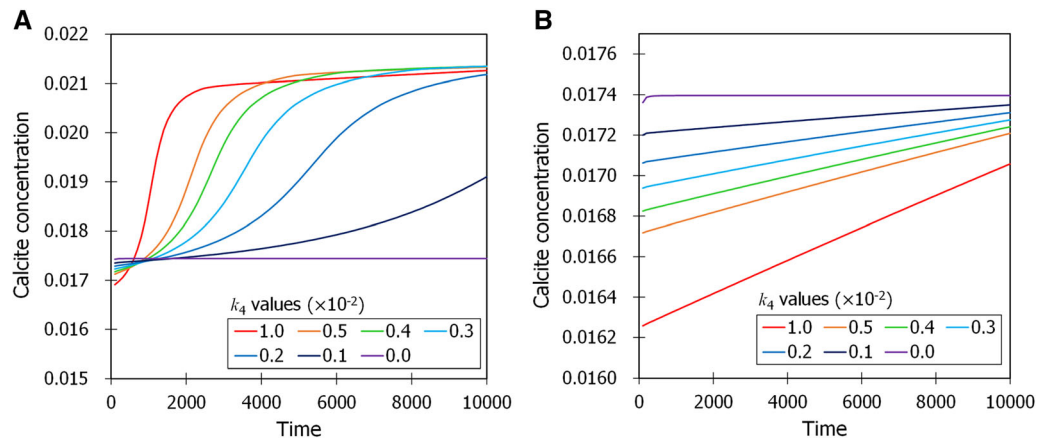
Fig. 6 The variation of calcite concentration with time in the non-diffusion type model. **a** The case of $k_1 = 25$, $k_2 = 0.005$, and $k_3 = 10$; **b** the case of $k_1 = 10$, $k_2 = 0.005$, and $k_3 = 25$. In the both calculations, the values of k_4 were set to 1.0×10^{-2}, 0.5×10^{-2}, 0.4×10^{-2}, 0.3×10^{-2}, 0.2×10^{-2}, 0.1×10^{-2}, and 0.0
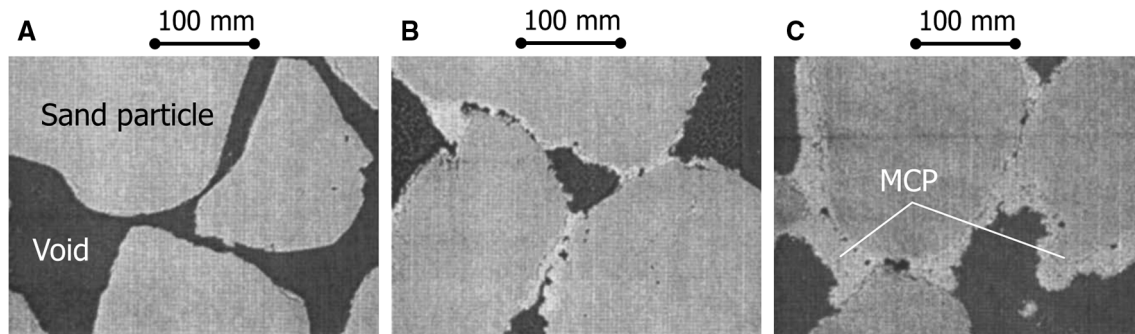

Fig. 7 Scanning electron microscopy images for microbial-induced solidified sand (modified from DeJong et al. [17]). The calcite cements are produced on the surfaces of sand particles and at void locations

strong resemblance between the precipitation patterns obtained by the proposed model and MCP features may be observed from the point of view of the morphological process of MCP spreading from soil particle surfaces to voids. The calcite precipitation on particle surfaces was observed in some experiments and in the simulations. It is of note that in these simulations, despite the identical analytical conditions of both the void fraction and particle surfaces, and therefore there were no specific boundary conditions on the particle surfaces, these concentration phenomena still occur. What is the cause of this concentrated calcite precipitation on soil particle surfaces and at soil particle contacts?

As shown in Fig. 3, calcite precipitation concentration was not observed on particle surfaces in the case for which no diffusion terms were used in Eqs. (3)–(8). These results indicate that MCP with the urea hydrolysis reaction may depend on diffusion. The calcium and carbonate ions are diffused into the whole region at the initial stage and remain at the particle boundaries. These ions then bind chemically onto the surface of particles where diffusion

stops. Figure 8 shows a conceptual illustration of the MCP process.

Let us consider the change in the amount of calcite precipitation. From Fig. 4a, we observe that calcite concentration increased as the value of k_4 decreased in the case for which $k_1 \leq k_3$. Clearly, there is a transition region between exponentially increasing areas in which the calcite concentration undergoes a significant change. In contrast, in the case for which $k_1 > k_3$ (see Fig. 4b), calcite concentration decreased as the value of k_4 decreased, and no significant shift in the calcite concentration was observed. These results suggest that the significant shift in the calcite concentration may depend on the calcification rate rather than the rate of the urea hydrolysis reaction described in Eq. (1). This implies that chemical inhibitors, the reverse reaction shown in Eq. (2), have a greater impact on these significant shifts than the activity of the microbial urea hydrolysis reaction. In addition, in the case for which $k_1 > k_3$, where the rate of microbial urea hydrolysis was larger than the calcification rate (see Fig. 6a), although some significant shifts were observed where diffusion terms were used, the gradual increase in calcite
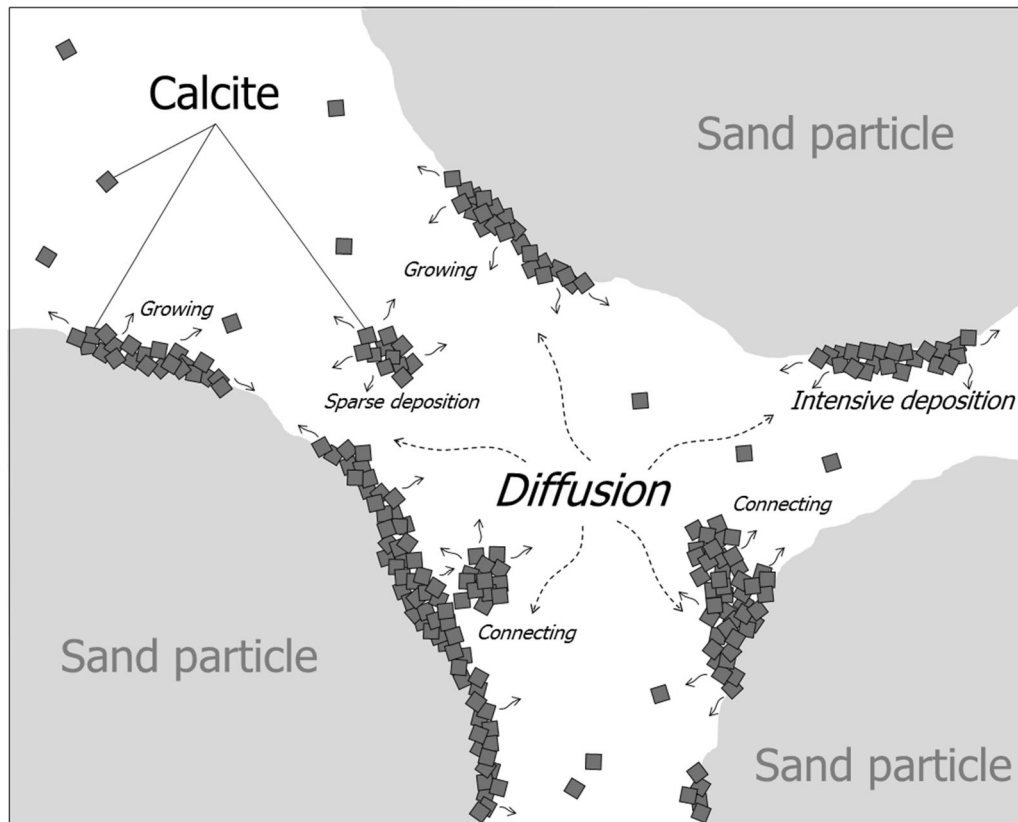
Fig. 8 Drawing of calcite precipitation after microbial urea hydrolysis. The calcite precipitations occur at void fractions and on the surfaces of grains, and some calcite precipitations are connected to each other. The surface precipitations depend on the diffusion of substances

concentration observed in laboratory experiments [18] cannot be confirmed. Hence, a value of $k_1 \leq k_3$ is one of the necessary conditions for realizing effective microbial carbonate precipitation. To date, it remained unclear whether or not the significant shifts in calcite concentration are caused by microbial expansion activity. The presented numerical analyses contained in this study have addressed and answered this question.

5 Conclusion

In the current work, a new mathematical model for microbial carbonate precipitation in the case of the urea hydrolysis reaction has been proposed, and a novel numerical simulator developed. Our interpretation of the simulation results may be summarized as follows:

1. The morphology of the precipitation patterns obtained by the proposed model closely resembles the features of MCP.
2. Although there are no specific boundary conditions on the particle surfaces, calcite precipitation on the particle surfaces is observed.

3. In MCP, the diffusion of each ion plays a very important role in the on-particle calcite precipitation.
4. Calcium and carbonate ions are diffused into the whole region, and these ions then bind chemically onto the surface of the particles, at which point diffusion halts.
5. Chemical inhibitors have a larger impact on the significant shifts in the calcite concentration compared to the activity of the microbial urea hydrolysis reaction.

It should be noted that the wide range of physical parameters given in this study should be determined experimentally. Additionally, in the proposed model, the distribution of bacterial population cannot be considered although the distribution may influence to reaction rate constant k_1 in Eq. (1). Also, calcium carbonate polymorphisms (calcite, vaterite, and aragonite) cannot be distinguished in the model because metastable transition of calcium carbonates cannot be considered though some complex transitions may be occurred in bio-cementation [2]. Hence, there is room for further improvement in the system. Although the proposed model is not the only possible scheme for understanding soil improvement due to MCP, this work describes a series of techniques that greatly support our understanding of microbial carbonate

precipitation at the microscale and provides the details of a novel method that may be applied to other similar processes.

References

1. Akiyama M, Kawasaki S (2019) Biogeochemical simulation of microbially induced calcite precipitation with *Pararhodobacter* sp. strain SO1. Acta Geotech 14(3):685–696

2. Al-Thawadi S, Cord-Ruwisch R (2012) Calcium carbonate crystals formation by ureolytic bacteria isolated from Australian soil and sludge. J Adv Sci Eng Res 2(1):12–26

3. Alvarez R, Steinbach HS (2009) A review of the effects of tillage systems on some soil physical properties, water content, nitrate availability and crops yield in the Argentine Pampas. Soil Tillage Res 104(2009):1–15

4. Ben-Jacob E, Cohen I, Shochet O, Aranson I, Levine H, Tsimring L (1995) Complex bacterial patterns. Nature 373(6515):566

5. Boore DM (2003) Simulation of ground motion using the stochastic method. Pure appl Geophys 160(2003):635–676

6. Boquet E, Boronat A, Ramos-Cormenzana A (1973) Production of calcite (calcium carbonate) crystals by soil bacteria is a general phenomenon. Nature 246(5434):527

7. Cambell CS, Cleary PW, Hopkins M (1995) Large-scale landslide simulations: global deformation, velocities and basal friction. J Geophys Res 100(B5):8267–8283

8. Chen W, Qie T (2011) Numerical simulations for large deformation of granular materials using smoothed particle hydrodynamics method. Int J Geomech 12(2):127–135

9. Cheng L, Shahin MA, Chu J (2019) Soil bio-cementation using a new one-phase low-pH injection method. Acta Geotech 14(3):615–626

10. Chou CW, Seagren EA, Aydilek AH, Lai M (2011) Biocalcification of sand through ureolysis. J Geotech Geoenviron Eng 137(12):1179–1189

11. Chu J, Ivanov V, Naeimi M, Stabnikov V, Liu HL (2014) Optimization of calcium-based bioclogging and biocementation of sand. Acta Geotech 9(2):277–285

12. Cil MB, Alshibli KA (2014) 3D analysis of kinematic behavior of granular materials in triaxial testing using DEM with flexible membrane boundary. Acta Geotech 9(2):287–298

13. Cohen I, Golding I, Kozlovsky Y, Ben-Jacob E, Ron IG (1999) Continuous and discrete models of cooperation in complex bacterial colonies. Fractals 7(03):235–247

14. Dadda A, Geindreau C, Emeriault F, du Roscoat SR, Garandet A, Sapin L, Filet AE (2017) Characterization of microstructural and physical properties changes in biocemented sand using 3D X-ray microtomography. Acta Geotech 12(5):955–970

15. Danjo T, Kawasaki S (2016) Microbially induced sand cementation method using *Pararhodobacter* sp. strain SO1, inspired by beachrock formation mechanism. Mater Trans 57(3):428–437

16. De Muynck W, De Belie N, Verstraete W (2010) Microbial carbonate precipitation in construction materials: a review. Ecol Eng 36(2):118–136

17. DeJong JT, Fritzges MB, Nüsslein K (2006) Microbially induced cementation to control sand response to undrained shear. J Geotech Geoenviron Eng 132(11):1381–1392

18. DeJong JT, Mortensen BM, Martinez BC, Nelson DC (2010) Biomediated soil improvement. Ecol Eng 36(2010):197–210

19. Desrues J, Chambon R, Mokni M, Mazerolle F (1996) Void ratio evolution inside shear bands in triaxial sand specimens studied by computed tomography. Géotechnique 46(3):529–546

20. Ek MB, Mitchell KE, Lin Y, Rogers E, Grunmann P, Koren V, Gayno G, Tarpley JD (2003) Implementation of Noah land surface model advances in the national centers for environmental prediction operational mesoscale Eta model. J Geophys Res 108(D22):8851

21. Fauriel S, Laloui L (2012) A bio-chemo-hydro-mechanical model for microbially induced calcite precipitation in soils. Comput Geotech 46(2012):104–120

22. Feng K, Montoya BM, Evans TM (2017) Discrete element method simulations of bio-cemented sands. Comput Geotech 85(2017):139–150

23. Gao Y, Hang L, He J, Chu J (2019) Mechanical behaviour of biocemented sands at various treatment levels and relative densities. Acta Geotech 14(3):697–707

24. Golding I, Kozlovsky Y, Cohen I, Ben-Jacob E (1998) Studies of bacterial branching growth using reaction–diffusion models for colonial development. Phys A 260(3–4):510–554

25. Hatanaka M, Feng L, Matsumura N, Yasu H (2008) A study on the engineering properties of sand improved by the sand compaction pile method. Soils Found 48(1):73–85

26. Hirose K, Matsubara H (2018) Mechanisms of mudcrack formation and growth in bentonite paste. J Geotech Geoenviron Eng 144(4):04018017

27. Horpibulsuk S, Miura N, Nagaraj TS (2005) Clay-water/cement ratio identity for cement admixed soft clays. J Geotech Geoenviron Eng 131(2):187–192

28. Hungr O (1995) A model for the runout analysis of rapid flow slides, debris flows, and avalanches. Can Geotech J 32(4):610–623

29. Iwashita K, Oda M (2000) Micro-deformation mechanism of shear banding process based on modified distinct element method. Powder Technol 109(2000):192–205

30. Kondo S, Miura T (2010) Reaction–diffusion model as a framework for understanding biological pattern formation. Science 329(5999):1616–1620

31. Konhauser KO (2007) Introduction to geomicrobiology. Wiley, Hoboken

32. Kozlovsky Y, Cohen I, Golding I, Ben-Jacob E (1999) Lubricating bacteria model for branching growth of bacterial colonies. Phys Rev E 59(6):7025

33. Lee KJ, McCormick WD, Pearson JE, Swinney HL (1994) Experimental observation of self-replicating spots in a reaction–diffusion system. Nature 369(6477):215

34. Matsushita M, Hiramatsu F, Kobayashi N, Ozawa T, Yamazaki Y, Matsuyama T (2004) Colony formation in bacteria: experiments and modeling. Biofilms 1(4):305–317

35. Matsushita M, Wakita J, Itoh H, Watanabe K, Arai T, Matsuyama T, Sakaguchi H, Mimura M (1999) Formation of colony patterns by a bacterial cell population. Phys A 274(1–2):190–199

36. McCutcheon J, Nothdurft DL, Webb EG, Shuster J, Nothdurft L, Paterson D, Southam G (2017) Building biogenic beachrock: visualizing microbially-mediated carbonate cement precipitation using XFM and a strontium tracer. Chem Geol 465:21–34

37. Mortensen BM, Haber MJ, DeJong JT, Caslake LF, Nelson DC (2011) Effects of environmental factors on microbial induced calcium carbonate precipitation. J Appl Microbiol 111(2):338–349

38. Okwadha GD, Li J (2010) Optimum conditions for microbial carbonate precipitation. Chemosphere 81(9):1143–1148

39. Oshiro H, Matsubara H (2018) Carbonate precipitation through photoautotrophic microorganisms at the Giza cliff in Okinawa, Japan. Environ Earth Sci 77:591

40. Pearson JE (1993) Complex patterns in a simple system. Science 261(5118):189–192

41. Rosen BP (1987) Bacterial calcium transport. Biochim Biophys Acta Rev Biomembr 906(1):101–110

42. Sakiyama H, Matsubara H (2018) Physical, chemical, and biological investigation of an unconformity between limestone and sandstone in a coastal area: Iriomote Island case study. CATENA 171(2018):136–144

43. Sánchez-Román M, Rivadeneyra MA, Vasconcelos C, McKenzie JA (2007) Biomineralization of carbonate and phosphate by moderately halophilic bacteria. FEMS Microbiol Ecol 61(2):273–284

44. Shen S, Chai J, Hong Z, Cai F (2005) Analysis of field performance of embankments on soft clay deposit with and without PVD-improvement. Geotext Geomembr 23(2005):463–485

45. Sun X, Miao L, Tong T, Wang C (2019) Study of the effect of temperature on microbially induced carbonate precipitation. Acta Geotech 14(3):627–638

46. Tagliaferri F, Waller J, Andò E, Hall SA, Viggiani G, Bésuelle P, DeJong JT (2011) Observing strain localisation processes in bio-cemented sand using x-ray imaging. Granul Matter 13(3):247–250

47. Terzis D, Laloui L (2018) 3-D micro-architecture and mechanical response of soil cemented via microbial-induced calcite precipitation. Sci Rep 8(1):1416

48. Terzis D, Laloui L (2019) Cell-free soil bio-cementation with strength, dilatancy and fabric characterization. Acta Geotech 14(3):639–656

49. Thompson JB, Ferris FG (1990) Cyanobacterial precipitation of gypsum, calcite, and magnesite from natural alkaline lake water. Geology 18(10):995–998

50. Turing AM (1952) The chemical basis of morphogenesis. Philos Trans R Soc Lond B Biol Sci 237(641):37–72

51. Whiffin VS, Paassen LA, Harkes MP (2007) Microbial carbonate precipitation as a soil improvement technique. Geomicrobiol J 24(2):417–423

52. White AF, Bullen TD, Vivit DV, Schulz MS, Clow DW (1999) The role of disseminated calcite in the chemical weathering of granitoid rocks. Geochim Cosmochim Acta 63(13–14):1939–1953

53. Więckowski Z (2004) The material point method in large strain engineering problems. Comput Methods Appl Mech Eng 193(39–41):4417–4438

54. Wu Y, Ajo-Franklin JB, Spycher N, Hubbard SS, Zhang G, Williams KH, Taylor J, Fujita Y, Smith R (2011) Geophysical monitoring and reactive transport modeling of ureolytically-driven calcium carbonate precipitation. Geochem Trans 12(1):7

55. Zhu T, Dittrich M (2016) Carbonate precipitation through microbial activities in natural environment, and their potential in biotechnology: a review. Front Bioeng Biotechnol 4:4